https://doi.org/10.1016/j.combustflame.2018.05.023

A theoretical kinetics study on Low-temperature reactions of methyl acetate radicals with molecular oxygen

Qinghui Meng, [a,b] Xudong Zhao, [a] Lidong Zhang, [a*] Peng Zhang, [b*] Liusi Sheng [a]

[a]*National Synchrotron Radiation Laboratory, University of Science and Technology of China, Hefei, Anhui 230029, P. R. China*

[b]*Departmental of Mechanical Engineering, the Hong Kong Polytechnic University, Hung Hom, Hong Kong*

Corresponding Author:
Lidong Zhang
National Synchrotron Radiation Laboratory
University of Science and Technology of China
Hefei, Anhui 230029, P.R. China
E-mail: zld@ustc.edu.cn
Fax: (86) 551 65141078 Tel: (86) 551 63607923

Peng Zhang
Department of Mechanical Engineering
The Hong Kong Polytechnic University
Kowloon, Hong Kong
E-mail: pengzhang.zhang@polyu.edu.hk
Fax: (852)23654703 Tel: (852)27666664

ABSTRACT

Theoratical studies on the chemistry of methyl acetate radicals with molecular oxygen was conducted to get further understanding of biodiesel combustion. Reaction networks of the first oxygen addition to methyl acetate radicals has been investigated by high level quantum chemical methods , and rate constants were computed by using microcanonical variational transition state theory coupled with Rice-Ramsberger-Kassel-Marcus/Master-Equation theory. The calculated rate constants agree reasonably well with both theoretical and experimental results of chain-like alkoxy radicals. We considered each step in the oxidation process as a class of reaction, including all the possible reactions taking place, only the formation and re-dissociation of initial adducts are critical for the low temperature combustion of methyl acetate. The current study is an extension of kinetic data for such chain branching and propagation reactions for methyl acetate oxidation in a wider pressure and temperature range, which can be used for the modeling study of low temperature oxidation of methyl esters.

Keywords: Methyl acetate, RRKM, Master equation, low-temperature oxidation, biodiesel

1. Introduction

Biodiesel, as an environment friendly source of renewable energy, has been regarded as one of the most promising alternative fuels [1-3]. The main component of biodiesel is esters, which contain oxygen in their molecular structure and can be obtained from several types of oil, including soybean oil in

the United States and rapeseed in Europe [4]. Esters are typically made of long (16-18) carbon atom chains and usually require very large detailed chemical kinetic models to precisely describe their oxidation. Compared with the combustion of fossil fuels, combustion of biodiesels could effectively reduce soot formation by suppressing its precursors in combustion processes [5], mitigating the climatic impact of fuel combustion. The detailed kinetic study of biodiesel is challenging both experimentally and theoretically because of the complexity and the size of the biodiesel components. As a result, surrogate molecules are widely used in kinetic studies to imitate the property of real biodiesel. Some small molecules, such as methyl formate, methyl acetate (MA), methyl crotanoate, and methyl butanoate (MB), have instead served as surrogates for studies of biodiesel recently [6-9].

MA is the simplest methyl ester with a chain only one carbon atom connected to the methyl ester group. MA is also an important reaction intermediate during the pyrolysis of biodiesel and a potential pollutant of the atmospheric degradation. Furthermore, association reactions of MA radicals and O_2 reaction represent an important model system to explore the kinetic consequences of the methyl ester radical oxidation; it contains many of the complexities of larger systems, yet is more feasible to detailed electronic structure calculations.

While the research on the high temperature oxidation and pyrolysis is extensive [10-13], only a few studies have been performed to promote the

development of low-temperature oxidation sub-mechanisms for methyl esters. A theoretical study of low-temperature oxidation of MB was conducted by Tao et al. [14], in which reaction channels, kinetics of methyl ester peroxy radical decomposition but the O_2 addition reaction were considered. Jiao et al. [15] investigated the autoignition of MB theoretically, and the study focused on the quantum chemistry and kinetics of second O_2 addition reactions to MB peroxy radicals. As for the oxidation reactions of MA, the first study was performed by Dagaut et al. [16] at temperature between 800 and 1230K, and a comprehensive kinetic mechanism was then developed to interpret the phenomena observed in JSR experiments. Recently, Deka et al. [17] developed a kinetic mechanism where the rate coefficient of the H-atom abstraction of MA by chlorine atoms was computed by using G2(MP2)//MPWB1K/6-31+G(d,p) method and RRKM master equation analysis at 298K. Tan et al. [18] also respectively conducted theoretical studies on the H-atom abstraction of MA initiated by free radicals (H, OH, HO_2, CH_3 and O), whose predications were validated against available theoretical results reported previously [11, 19].

Many studies have been conducted on the hydrogen abstraction of MA [18, 19]. Few studies focused on the sub-mechanism of low-temperature oxidation for MA. The ignition of MA is mainly initiated by hydrogen abstraction with free radicals to form one of two carbon centered radicals: $\cdot CH_2COOCH_3$ (denoted by MA2J) and $CH_3COOCH_2\cdot$ (denoted by MAMJ). The MA radicals can isomerize to each other via 1, 4-H shift. Under low temperature range, MA

radicals can directly react with O_2 and then form peroxy radicals. These peroxy radicals can isomerize to hydroperoxy alkyl radicals (·QOOH), which in turn can decompose through concerted OH-loss or β-scission and can reverse to the peroxy radicals. The OH-loss and β-scission reactions involving ·QOOH either propagate the radical chain reaction or lead to radical chain branching. These reactions have a great influence on the low-temperature combustion chemistry of MA. Compared with the analogous alkyl reaction systems, the present system is more complicated because of the presence of the oxygenated ester group.

In the manuscript, MA is recognized as a candidate methyl ester for surrogate formulation, and is also considered as the starting point for the development of reaction rate rules and kinetic mechanism of other methyl esters. For the present work, we identified detailed reaction pathways for each radical and determined the potential energy surfaces (PES) by using highly accurate theoretical methods. Rate constants were subsequently calculated for dominant channels. Master equation analysis of the kinetics for barrierless reactions was performed to obtain accurate temperature- and pressure-dependent rate constants. Moreover, phenomenological rate coefficients and competing relationship among reaction pathways were provided for this system to develop the chemical kinetic modelling of low temperature oxidation of methyl esters. A detailed kinetic model of reactions of

MA peroxy radicals and QOOH has been described in the present study which is also compared with MB peroxy radicals reported in early studies [14].

2. Theoretical Methodology

2.1 Electronic structure calculations

The method of M06-2X/cc-pVTZ was employed in the geometry optimization and frequency analysis of stationary points on the MAOO potential energy surfaces [20]. Transition states possessing one and only one imaginary frequency were verified to correspond to desired reaction coordinates via visual inspections. For ambiguous cases, the intrinsic reaction path analysis was utilized to examine the connections of each saddle point to its local minima. Vibrational frequencies were scaled by a factor of 0.985 [21], and the zero-point energies (ZPE) were obtained at M06-2X/cc-pVTZ level. High level single-point energies of these species were corrected by using two high-level theories. The first one is the coupled-cluster singles and doubles with perturbative triples correction (CCSD(T)) theory implemented in Molpro package [22]. The single-point energies were obtained by restricted CCSD (T) with cc-pVXZ (X= D, T) basis sets [23]. The second is the explicitly-corrected CCSD(T)-F12 method [24] implementation in the same package [22]. The extrapolation of F12 correlation energies can be highly accurate even with just a DZ/TZ pair of basis sets [24]. Energy extrapolation to the complete basis set (CBS) limit was conducted with two-point extrapolation scheme [23, 24]:

$E[CCSD(T)/CBS]_{DZ\rightarrow TZ}$

= E[CCSD(T)/cc-pVTZ]

+{E[CCSD(T)/cc-pVTZ]-E[CCSD(T)/cc-pVDZ]}×0.4629 (E1)

$E[CCSD(T)\text{-}F12/CBS]_{DZ\rightarrow TZ}$

= E[CCSD(T)-F12/cc-pVTZ]

+{E[CCSD(T)-F12/cc-pVTZ]

-E[CCSD(T)-F12/cc-pVDZ]}×0.4210 (E2)

The molecular oxygen with triple ground state reacts like radicals in the entrance channel of O_2 addition reactions that are typically barrierless. Single reference methods failed to deal with this process. Thus, the multi-reference method CASSCF(7e,5o)/cc-pVDZ-F12 was employed for frequency calculations and the relaxed scan along the reaction coordinate. The active space was chosen as (7e, 5o) including six electrons in two pairs of O-O π and π* orbitals and one electron in a radical orbital. After that, the explicitly correlated multi-reference configuration interaction (MRCI-F12) method combined with the cc-pVDZ-f12 basis set was used to map out the minimum energy pathway (MEP) [25].When combined with cc-pVDZ-F12 orbital auxiliary basis sets, recently developed F12 methods utilize an exponential correlation factor, which can achieve results near aug-cc-pVQZ quality with a negligible increase in computation load [26, 27]. The energy obtained above were scaled asymptotically by referring to corresponding energies of the O_2 addition reactions achieved at CCSD(T)/CBS//M06-2X/cc-pVTZ level.

For the barrierless channels in this case, the CASPT2 method is unable to predict smooth energy potentials due to the existence of strong interactions between O and H atoms. An H atom could even be abstracted by O_2 with these two atoms getting closed to each other, which is also found in previous studies [28]. Thereby, the potential calculations by using the MRCI-F12(7e,5o)/cc-pVDZ-F12//CASSCF(7e,5o)/cc-pVDZ-F12 were chosen for the O_2 addition channels.

All the present DFT calculations were performed by using the Gaussian 09 program suite [29]; multi-reference calculations were performed by using the Molpro 2010 program package [22].

2.2 Rate constant calculations

The pressure-dependent rate coefficients were computed though solving the time-dependent master equations based on RRKM theory [30] by employing the MESS code [31]. The collisional energy transfer was approximated by a single-exponential-down model, $(\Delta E)_{down}=250(T/300K)^{0.85}$, which has been validated in relevant studies of MB [32] and n-butyl radicals [33]. Rate constant calculations were performed for wide ranges of temperatures from 300 to 1500 K and pressures from 0.01 atm to 100 atm. The interaction between reactant and bath gas Argon was estimated by using the Lennard–Jones (L–J) model. The L-J parameters of Ar, σ = 3.47 Å and ε = 79.2 cm^{-1}, were adopted from the early literature [34]. For methyl acetate radicals, the L-J parameters, σ =5.94 Å

and $\varepsilon = 669.8\ cm^{-1}$, were calculated by using the empirical method of Chung et al. [35, 36].

For the channels with pronounced transition states, the high-pressure rate constants were computed by using the conventional transition state theory (CTST) applying the rigid-rotor harmonic-oscillator (RRHO) assumption for all degrees of freedom except for the torsional modes. The low-frequency torsional modes corresponding to internal rotations were simulated as one-dimensional (1-D) hindered rotors with hindrance potentials, which were obtained by a relaxed scan with the increment of 10 degrees at the M06-2X/cc-pVTZ level. As reactions considered in the consumption of MD radicals involving the transfer of hydrogen atoms, the tunnelling effect on the rate constants was calculated on base of asymmetric Eckart model [37].

On MAOO surfaces, the O_2 addition reaction to MA radicals has a loose transition state along the reaction coordinate and the microcanonical variational transition state theory (μVTST) was implemented to evaluate the minimum number of states at each specific energy for the transition states [38, 39]. The most distinctive feature of μVTST approach lies in that the optimal dividing surface, which is devised to minimize the rate flux from reactants to products, is a function of energy [40, 41]. This procedure for computing variational TST rate constants was proposed by da Silva and Bozzelli [42]. As described above, the interaction potentials predicted by

MRCI-F12(7e,5o)/cc-pVDZ-F12//CASSCF(7e,5o)/cc-pVDZ-F12 were used in the variation treatment of transition state theory.

3 Results and discussion

3.1 Electronic structure calculations

The MAOO radicals were generated from MA radicals with molecular oxygen via barrierless reaction channels. Optimized geometries, rotational constants and vibrational frequencies of all the species are given in the Supplementary Material. Table 1 display the well depth of the formation for MAOO adducts and their energy barriers of isomerization at 0K for the different O_2 addition reactions. Two independent theories of CCSD(T) and CCSD(T)-F12 were utilized to calculate the single-point energies of all the species, and the results are almost the same between the two theories. Considering the calculation accuracy and computation cost, the PESs were constructed by using CCSD(T) theory. The M06-2X/cc-pVTZ optimized structures for the MAOO complexes produced by the addition of O_2 to MA radicals are illustrated in Figure S1. The lowest energy conformer of each MAOO radicals was identified as the local minimum though relaxed potential scans. These conformations were used as starting points when interaction potentials of barrierless reactions were explored by using MRCI-F12 method implemented in Molpro [22].

The PES for the major reaction channels at the CCSD(T)/CBS//M06-2X/cc-pVTZ level is shown in Figure 1. The well depths

of the initially-formed adducts, such as MA2JOO and MAMJOO are 24.33 and 32.94 kcal/mol, respectively. The energy barrier of MA2J is significantly lower than that of MAMJ owing to the presence of –C(·)-C=O- conjugated system in the MA2J radical, which reduces the energy of MA2J +O_2 and therefore has different reaction behaviours. The well depth of MAOO· adduct determines how the re-dissociation channel competes with other decomposition reaction channels of MAOO. The initial adduct MA2JOO isomerizes to form $CH_2(OOH)C(=O)CH_2$· (i.e. W2 in Fig. 1) through a 7-membered-ring transition states with a barrier energy of 31.23 kcal/mol, which is higher than that of the re-dissociation of MA2JOO radicals (i.e. W1 in Fig. 1). Thus the re-dissociation of W1 is more competitive that the isomerization. The MA2JOO adduct also can isomerizes to form $CH_2(OOH)C·(=O)CH_2$ via 1,3-H shift with a barrier of 40.38 kcal/mol (a relatively high energy), so its contribution to products is negligible. The intermediate W2, having the relative energy of -15.13kcal/mol, can undergo β-scission to form $HOOCH_2C·(=O)$ (i.e. P3 in Fig. 1) subsequently releasing a formaldehyde with a relative high barrier of 36.39 kcal/mol, this dissociation channel plays a less important role in the low-temperature oxidation of MA. The formation of $OCH_2C(=O)OCH_2OH$ (i.e. P4 in Fig. 1) goes through the OH-migration from MA2JOO with the high barrier of 40.38 kcal/mol. Even the product of OH-migration channel has a low relative energy, this channel is less important. Alternatively, the intermediate W2 can dissociate to form $CH(=O)C(=O)OCH_3$+OH. The lowest energy

reaction channel of this system is the formation of cy[$OCH_2C(=O)OCH_2$] via a 5-membered-ring transition state involving O-O bond breaking and C-O bond forming, with a barrier height of 21.18 kcal/mol.

For MAMJ +O_2 reaction system, the well depth of MAMJOO adduct formation is 32.94 kcal/mol lower than the reactants which are closer to those of MB system [14]. Two different products: cy[$C(=O)OCH_2OO$](P6′)+CH_3·, $CH_2C(=O)OO$· (P5′)+CH_2O can be directly formed from the initial adduct through ring TS, with barrier of 33.44 and 35.90 kcal/mol, respectively. The MAMJOO(W1′) can isomerize to form $CH_2C(=O)CH_2OOH$(W2′) via 1,6-H shift and $CH_3C(=O)OCHOOH$ via 1,3-H shift with the barrier of 33.86 and 42.29 kcal/mol, respectively. The product of this 1, 3-H shift isomerization is unstable and easily dissociate to form $CH_3C(=O)OCHO$(P4′)+OH. The $CH_2C(=O)CH_2OOH$(W2′) can dissociate to form cy[$OCH_2C(=O)OCH_2$](P1′)+OH and P4′+OH, with barrier of 27.74 and 30.57 kcal/mol, respectively. These four reaction channels are more favoured due to the lower barrier. A more detailed depiction can be discussed in rate constant analysis. These molecular properties of methyl acetate radical system can be applied to similar methyl ester oxidation systems in the later related studies.

3.2 High-pressure limit rate constants

Because of the paucity of kinetics data of methyl acetate, only comparisons with previous high-pressure rate constants of chain-like radicals were made for

the present system. Only the kinetically preferred reaction pathways discussed above were taken into consideration for rate constant calculations.

Figure 2 represent the present prediction of high pressure limit rate constants for the O_2 addition to methyl acetate radicals by using the variational transition state theory. From the plots, addition reactions of O_2 to methyl acetate radicals show positive temperature dependence, which is also reported in the reaction of ethyl and O_2 by Miller et al. [38]. At temperature below 800K, the recombination rate constant of MA2J + O_2 is higher than that of MAMJ+ O_2, which is attributed to the lower well depth at low temperatures. The recombination rate constant of the MAMJ + O_2 show slightly positive temperature dependence. At low temperatures, the variational transition state locates at shorter C-O distance, where the MEP has a large slope and the enthalpy change dominates the temperature dependence. As temperature increases, the transition state lies at longer C-O separation where the MEP has a smaller slope and the decreasing entropy dominates the temperature dependence. Compared with the MA2J system, the transition state of MAMJ+O_2 lies at a longer C-O distance and the rate constants rise slightly with the increase of temperature. For O_2 addition to the MAMJ, the rate constants are larger than those of MA2J in the important range of low temperature (500-800 K), which displays weaker temperature dependence. Due to the uniqueness of methyl acetate and scarcely available data, rate constants of low oxidation reactions for ether [43] and ethyl [38] were illustrated for comparison.

The association rate constant of ethyl and O_2 demonstrated relatively comparable temperature dependence with that of MAMJ and O_2, while deviations are as high as two orders of magnitude [38]. This is because association reactions of MAMJ and O_2 with resonance interaction have swallower well depth than that of ethyl systems by 1.1 kcal/mol [38].

The low-temperature oxidation kinetic data of n- and i-propoxy radicals and O_2 have been measured by Fittschen et al. [44] though experimental detection, which are in generally good agreement with our results at temperature between 300 and 500K. in addition, association rate constants of i-propoxy radicals and O_2 explored by Setokuchi et al. [43] on base of the high-level ab initio theory and the variational transition state theory, agree well with the present calculations at temperature ranging from 300 to 1500K.

3.3 Pressure-dependent rate constants

It is recognized that reaction mechanisms of ROO radicals do significant effect on the autoignition behaviour of biodiesels [45]. In the present problem, the temperature and pressure-dependent kinetics is sensitive to the well depth of the MAOO formation. Figure 3 plots recombination rate constants of MAOO+ O_2 at different pressures. Below 600 K, the calculated rate constants show weakly pressure dependent, while significant pressure dependence was observed with temperature increase. For example, rate constants show a factor of 2 orders of magnitude deviation at 0.01 atm and 1000 K, comparing with that of high pressure limit. At 0.01 atm, absence of rate constants at temperature

above 700 K is explained by the fact that the MA2JOO equilibrates with W1 more rapidly than its collisional energy transfer. There is a fall-off at finite pressures as the stabilization reaction equilibrates, and the onset temperature increases with the pressures. The complex behaviour is attributable to the dissociation mechanism of MAOO to MA + O_2.

Intramolecular hydrogen transfer is a key step for low-temperature oxidation reactivity of fuels. Figure 4 demonstrates rate constants and of isomerization reactions for MA radicals, with relevant data of MB and dimethyl ether for comparison. In the present system, the products of 1, 3- H shift with relatively high barrier height is hard to proceed, and therefore only the kinetic parameters of 1, 6-H shift for MAOO radicals were considered in this manuscript. The rate constant of 1, 6-H shift for MA2JOO is higher than that of MAMJOO by a rough factor of 10 due to the lower energy barrier. As shown in Figure 4, the calculated rate constants of isomerization reactions for MBOO are in excellent agreement with the theoretical data predicted by using G3MP2B3//B3LYP/6-31G(d)method [14] except for isomerization reactions from MBMJOO radicals at low temperature. At temperature below 800 K, kinetic difference between 1, 6-H migration reactions of MBMJOO and that of MAMJOO is as high as 5 orders of magnitude, which is caused by the fact that MBMJOO isomerization reaction with barrier height of 29 kcal/mol is roughly lower than that of MAMJOO by 4 kcal/mol. In addition, the rate constant of

MAMJOO isomerization has a good agreement with that of dimethyl ether peroxy adduct, which has an O atom in the ring-structure transition state [46].

To clearly clarify the relationship at various regimes (T/P), Figures 5 and 6 display the temperature and pressure effect on the rate constants of main channels for two different systems. For simplicity, only rate constants at pressure of 0.01atm and 10atm were depicted in Figures 5 and 6. The respective branching ratio of the production of MA2JOO and MAMJOO is sum up to 99% or more, indicating that the rate constants of stabilization reactions is 99% of the overall rate constant.

It is evident that the re-dissociation reaction of MA2JOO is the most important channel and the OH elimination reaction is secondary, as shown in Figure 5. Here the kinetic results confirm the observations made from the PES in Figure 1. Our calculation shows that the isomerization is not comparable with the re-dissociation reaction of MA2JOO radicals and the contribution of OH migration channel is negligible at low temperature. Both thermally and chemically activated formation of products become energetic and the formation of cyclic pathway is more competitive. The rate constant of stabilization reaction channel increases with pressure. Absence of rate constants at higher temperature is caused by multi-well reduction adopted in the MESS code. Furthermore, the rate constants of product channels decrease with increasing the pressure, and the similar trend for the O_2 addition to chain-like alkyl radical was observed. Comparing with other remaining channels, the rate constant of cyclization channel decreases faster. As shown in Figure 6, the rate constant of the

association reaction is the most favoured reaction at the beginning stage and that of the isomerization reaction to W1' is the secondary, which is consistent with the prediction based on PES in Figure 1. With increasing pressure, the stabilization channel approaches the high-pressure limit at higher temperature. The rate constants of other channels generally decrease with increasing pressure. After O_2 addition reaction, these four channels competitive with each other subsequently. Our calculations show that the well depth of the initial adduct has great influence on the rate constants of consequent reactions. The dominant reaction channel is the formation of the initial adduct MAMJOO， as we anticipated. The reaction channel of aldehyde +OH formation is more competitive due to lower energy barrier. The rate constant of formaldehyde compounds channel is larger than that of isomerization, which can be attributed to the lower barrier heights of formaldehyde compounds channel. The isomerization and subsequent reaction channel play less important role in this system. The different temperature and pressure dependence observed in this system are consistent with the above discussion.

4 Conclusions

In the present study, we theoretically explored the sub-mechanism of oxidative reaction of methyl acetate at low temperatures. The potential energy surfaces for methyl acetate radicals $+O_2$ systems were delineated at the CCSD(T)/CBS level. Phenomenological rate constants for low temperature oxidation of methyl acetate radicals were performed on base of RRKM/ME

theory. Kinetic parameters of the association reactions were predicted using the microcanonical variational transition state theory. Present results of methyl acetate radicals agree well with limited available experimental and theoretical data. The detailed reaction sub-mechanism was constructed for the low-temperature oxidation and the autoignition of methyl ester. In summary, the mechanism of the MA2J+O_2 and MAMJ+O_2 system is similar excerpt for the stabilization channel. The dominant channel is the formation of initial adducts which are more competitive at low temperature and high pressure. To a great extent, the observed discrepancies of kinetics can be attributed to the different reaction enthalpies. Predicted kinetic data at various temperature and pressure of low-temperature oxidation of methyl acetate radicals provide a wider range of competing relationship between chain branching and chain propagation reactions, which can be helpful to improve the chemical kinetic modelling of methyl acetate oxidation.

Acknowledgements

The work at University of Science and Technology of China was supported by, National Key Scientific Instruments and Equipment Development Program of China (2012YQ22011305), and Natural Science Foundation of China (51676176, U1532137, 11575178 and 21373193). The work at the Hong Kong Polytechnic University was supported by RGC/ECS (PolyU 5380/13E), SRFDP & RGC ERG Joint Research Scheme (M-PolyU509/13), and NSFC (91641105). The authors thank the

supercomputing service of the Supercomputing Center of University of Science and Technology of China.

References:

[1] A.K. Agarwal, Biofuels (alcohols and biodiesel) applications as fuels for internal combustion engines, Prog. Energy Combust. Sci. 33 (2007) 233-271.
[2] J.Y.W. Lai, K.C. Lin, A. Violi, Biodiesel combustion: Advances in chemical kinetic modeling, Prog. Energy Combust. Sci. 37 (2011) 1-14.
[3] K. Kohse-Höinghaus, P. Oßwald, T.A. Cool, T. Kasper, N. Hansen, F. Qi, C.K. Westbrook, P.R. Westmoreland, Biofuel Combustion Chemistry: From Ethanol to Biodiesel, Angew. Chem. Int. 49 (2010) 3572-3597.
[4] L.C. Meher, D. Vidya Sagar, S.N. Naik, Technical aspects of biodiesel production by transesterification—a review, Renew. Sust. Energ. Rev. 10 (2006) 248-268.
[5] Q. Feng, A. Jalali, A.M. Fincham, Y.L. Wang, T.T. Tsotsis, F.N. Egolfopoulos, Soot formation in flames of model biodiesel fuels, Combust. Flame 159 (2012) 1876-1893.
[6] L. Yang, J.-y. Liu, Z.-s. Li, Theoretical Studies of the Reaction of Hydroxyl Radical with Methyl Acetate, J. Phys. Chem. A 112 (2008) 6364-6372.
[7] J.J. Orlando, G.S. Tyndall, The atmospheric oxidation of ethyl formate and ethyl acetate over a range of temperatures and oxygen partial pressures, Int. J. Chem. Kinet. 42 (2010) 397-413.
[8] K.-Y. Lam, D.F. Davidson, R.K. Hanson, High-temperature measurements of the reactions of OH with small methyl esters: methyl formate, methyl acetate, methyl propanoate, and methyl butanoate, J. Phys. Chem. A 116 (2012) 12229-12241.
[9] X. Zhou, Y. Zhai, L. Ye, L. Zhang, Theoretical studies on the reaction kinetics of methyl crotonate with hydroxyl radical, Sust. Energ. Fuels, Doi:10.1039/C7SE00426E(2018).
[10] S.L. Peukert, R. Sivaramakrishnan, M.C. Su, J.V. Michael, High temperature rate constants for H/D+methyl formate and methyl acetate, Proc. Combust. Inst. 34 (2013) 463-471.
[11] S.L. Peukert, R. Sivaramakrishnan, M.-C. Su, J.V. Michael, Experiment and theory on methylformate and methylacetate kinetics at high temperatures: Rate constants for H-atom abstraction and thermal decomposition, Combust. Flame 159 (2012) 2312-2323.
[12] X. Yang, D. Felsmann, N. Kurimoto, J. Krüger, T. Wada, T. Tan, E.A. Carter, K. Kohse-Höinghaus, Y. Ju, Kinetic studies of methyl acetate pyrolysis and oxidation in a flow reactor and a low-pressure flat flame using molecular-beam mass spectrometry, Proc. Combust. Inst. 35 (2015) 491-498.
[13] W. Ren, K.-Y. Lam, D.F. Davidson, R.K. Hanson, X. Yang, Pyrolysis and oxidation of methyl acetate in a shock tube: A multi-species time-history study, Proc. Combust. Inst. 36 (2017) 255-264.
[14] H. Tao, K.C. Lin, Kinetics and thermochemistry of methyl-ester peroxy radical decomposition in the low-temperature oxidation of methyl butanoate: A computational study of a biodiesel fuel surrogate, Combust. Flame 161 (2014) 2270-2287.
[15] Y. Jiao, F. Zhang, T.S. Dibble, Quantum Chemical Study of Autoignition of Methyl

Butanoate, J. Phys. Chem. A 119 (2015) 7282-7292.
[16] C.N. R. S, Methyl Acetate Oxidation in a JSR: Experimental and Detailed Kinetic Modeling Study, Combust. Sci. Technol. 127 (1997) 275-291.
[17] R.C. Deka, B.K. Mishra, A theoretical investigation on the kinetics, mechanism and thermochemistry of gas-phase reactions of methyl acetate with chlorine atoms at 298K, Chem. Phys. Lett. 595-596 (2014) 43-47.
[18] T. Tan, X. Yang, C.M. Krauter, Y. Ju, E.A. Carter, Ab Initio Kinetics of Hydrogen Abstraction from Methyl Acetate by Hydrogen, Methyl, Oxygen, Hydroxyl, and Hydroperoxy Radicals, J. Phys. Chem. A 119 (2015) 6377-6390.
[19] S. Jørgensen, V.F. Andersen, E.J.K. Nilsson, O.J. Nielsen, M.S. Johnson, Theoretical study of the gas phase reaction of methyl acetate with the hydroxyl radical: Structures, mechanisms, rates and temperature dependencies, Chem. Phys. Lett. 490 (2010) 116-122.
[20] Y. Zhao, D.G. Truhlar, The M06 suite of density functionals for main group thermochemistry, thermochemical kinetics, noncovalent interactions, excited states, and transition elements: two new functionals and systematic testing of four M06-class functionals and 12 other functionals, Theor. Chem. Acc. 120 (2008) 215-241.
[21] I.M. Alecu, J. Zheng, Y. Zhao, D.G. Truhlar, Computational Thermochemistry: Scale Factor Databases and Scale Factors for Vibrational Frequencies Obtained from Electronic Model Chemistries, J. Chem. Theory Comput. 6 (2010) 2872-2887.
[22] H. Werner, P. Knowles, G. Knizia, F. Manby, M. Schütz, P. Celani, T. Korona, R. Lindh, A. Mitrushenkov, G. Rauhut, See http://www. molpro. net.
[23] D. Feller, D.A. Dixon, Extended benchmark studies of coupled cluster theory through triple excitations, J. Chem. Phys. 115 (2001) 3484-3496.
[24] J.G. Hill, K.A. Peterson, G. Knizia, H.J. Werner, Extrapolating MP2 and CCSD explicitly correlated correlation energies to the complete basis set limit with first and second row correlation consistent basis sets, J. Chem. Phys. 131 (2009) 194105.
[25] T. Shiozaki, G. Knizia, H.J. Werner, Explicitly correlated multireference configuration interaction: MRCI-F12, J. Chem. Phys. 134 (2011) 034113.
[26] K.A. Peterson, T.B. Adler, H.-J. Werner, Systematically convergent basis sets for explicitly correlated wavefunctions: The atoms H, He, B–Ne, and Al–Ar, J. Chem. Phys. 128 (2008) 084102.
[27] K.E. Yousaf, K.A. Peterson, Optimized complementary auxiliary basis sets for explicitly correlated methods: aug-cc-pVnZ orbital basis sets, Chem. Phys. Lett. 476 (2009) 303-307.
[28] L. Ye, L. Zhang, F. Qi, Ab initio kinetics on low temperature oxidation of iso-pentane: The first oxygen addition, Combust. Flame 190 (2018) 119-132.
[29] M. J. Frisch; G. W. Trucks; H. B. Schlegel; G. E. Scuseria; M. A. Robb; J. R. Cheeseman; G. Scalmani; V. Barone; B. Mennucci; G. A. Petersson; H. Nakatsuji; M. Caricato; X. Li; H. P. Hratchian; A. F. Izmaylov; J. Bloino; G. Zheng; J. L. Sonnenberg; M. Hada; M. Ehara; K. Toyota; R. Fukuda; J. Hasegawa; M. Ishida; T. Nakajima; Y. Honda; O. Kitao; H. Nakai; T. Vreven; J. J. A. Montgomery; J. E. Peralta; F. Ogliaro; M. Bearpark; J. J. Heyd; E. Brothers; K. N. Kudin; V. N. Staroverov; T. Keith; R. Kobayashi; J. Normand; K. Raghavachari; A. Rendell; J. C. Burant; S. S. Iyengar; J. Tomasi; M. Cossi; N. Rega; J. M. Millam; M. Klene; J. E. Knox; J. B. Cross; V. Bakken; C. Adamo; J. Jaramillo; R. Gomperts; R. E. Stratmann; O. Yazyev; A. J. Austin; R. Cammi; C. Pomelli; J. W. Ochterski; R. L. Martin; K. Morokuma; V.

G. Zakrzewski; G. A. Voth; P. Salvador; J. J. Dannenberg; S. Dapprich; A. D. Daniels; O. Farkas; J. B. Foresman; J. V. Ortiz; J. Cioslowski; D. J. Fox, Gaussian 09, Revision D.01 ed.
[30] S.J. Klippenstein, J.A. Miller, From the Time-Dependent, Multiple-Well Master Equation to Phenomenological Rate Coefficients, J. Phys. Chem. A 106 (2002) 9267-9277.
[31] Y. Georgievskii, J.A. Miller, M.P. Burke, S.J. Klippenstein, Reformulation and Solution of the Master Equation for Multiple-Well Chemical Reactions, J. Phys. Chem. A 117 (2013) 12146-12154.
[32] L. Zhang, Q. Chen, P. Zhang, A theoretical kinetics study of the reactions of methylbutanoate with hydrogen and hydroxyl radicals, Proc. Combust. Inst. 35 (2015) 481-489.
[33] P. Zhang, S.J. Klippenstein, C.K. Law, b Initio Kinetics for the Decomposition of Hydroxybutyl and Butoxy Radicals of n-Butanol, J. Phys. Chem. A 117 (2013) 1890-1906.
[34] H. Hippler, J. Troe, H. Wendelken, Collisional deactivation of vibrationally highly excited polyatomic molecules. II. Direct observations for excited toluene, J. Chem. Phys. 78 (1983) 6709-6717.
[35] T.H. Chung, M. Ajlan, L.L. Lee, K.E. Starling, Generalized multiparameter correlation for nonpolar and polar fluid transport properties, Ind. Eng. Chem. Res. 27 (1988) 671-679.
[36] T.H. Chung, L.L. Lee, K.E. Starling, Applications of kinetic gas theories and multiparameter correlation for prediction of dilute gas viscosity and thermal conductivity, Ind. Eng. Chem. Fundam. 23 (1984) 8-13.
[37] C. Eckart, The penetration of a potential barrier by electrons, Phys. Rev. 35 (1930) 1303-1309.
[38] J.A. Miller, S.J. Klippenstein, S.H. Robertson, A theoretical analysis of the reaction between ethyl and molecular oxygen, Proc. Combust. Inst. 28 (2000) 1479-1486.
[39] J.A. Miller, S.J. Klippenstein, The reaction between ethyl and molecular oxygen II: Further analysis, Int. J. Chem. Kinet. 33 (2001) 654-668.
[40] S.J. Klippenstein, An efficient procedure for evaluating the number of available states within a variably defined reaction coordinate framework, J. Chem. Phys. 98 (1994) 11459-11464.
[41] J.A. Miller, Theory and modeling in combustion chemistry, Proc. Combust. Inst. 26 (1996) 461-480.
[42] G. da Silva, J.W. Bozzelli, Variational Analysis of the Phenyl + O2 and Phenoxy + O Reactions, J. Phys. Chem. A 112 (2008) 3566-3575.
[43] O. Setokuchi, M. Sato, Direct Dynamics of an Alkoxy Radical (CH3O, C2H5O, and i-C3H7O) Reaction with an Oxygen Molecule, J. Phys. Chem. A 106 (2002) 8124-8132.
[44] C. Fittschen, A. Frenzel, K. Imrik, P. Devolder, Rate constants for the reactions of C2H5O, i‐C3H7O, and n‐C3H7O with NO and O2 as a function of temperature, Int. J. Chem. Kinet. 31 (1999) 860-866.
[45] J. Zádor, C.A. Taatjes, R.X. Fernandes, Kinetics of elementary reactions in low-temperature autoignition chemistry, Prog. Energy Combust. Sci. 37 (2011) 371-421.
[46] T. Yamada, J.W. Bozzelli, T. Lay, Thermodynamic and kinetic analysis using AB initio calculations on dimethyl-ether radical+O2 reaction system, Proc. Combust. Inst. 27 (1998) 201-209.

Table 1. Comparison of the relative energies of various reaction channels calculated at 0 K by CCSD(T) and CCSD(T)-F12 methods

	$E_{CCSD(T)/CBS}$ (kcal/mol)	$E_{CCSD(T)-F12/CBS}$ (kcal/mol)
$\cdot CH_2COOCH_3+O_2 \rightarrow \cdot OOCH_2COOCH_3$	24.33	24.46
$CH_3COOCH_2\cdot+O_2 \rightarrow CH_3COOCH_2OO\cdot$	32.94	33.13
$\cdot OOCH_2COOCH_3 \rightarrow HOOCH_2COOCH_2\cdot$	31.23	31.15
$CH_3COOCH_2OO\cdot \rightarrow \cdot H_2CCOOCH_2OOH$	33.57	33.85

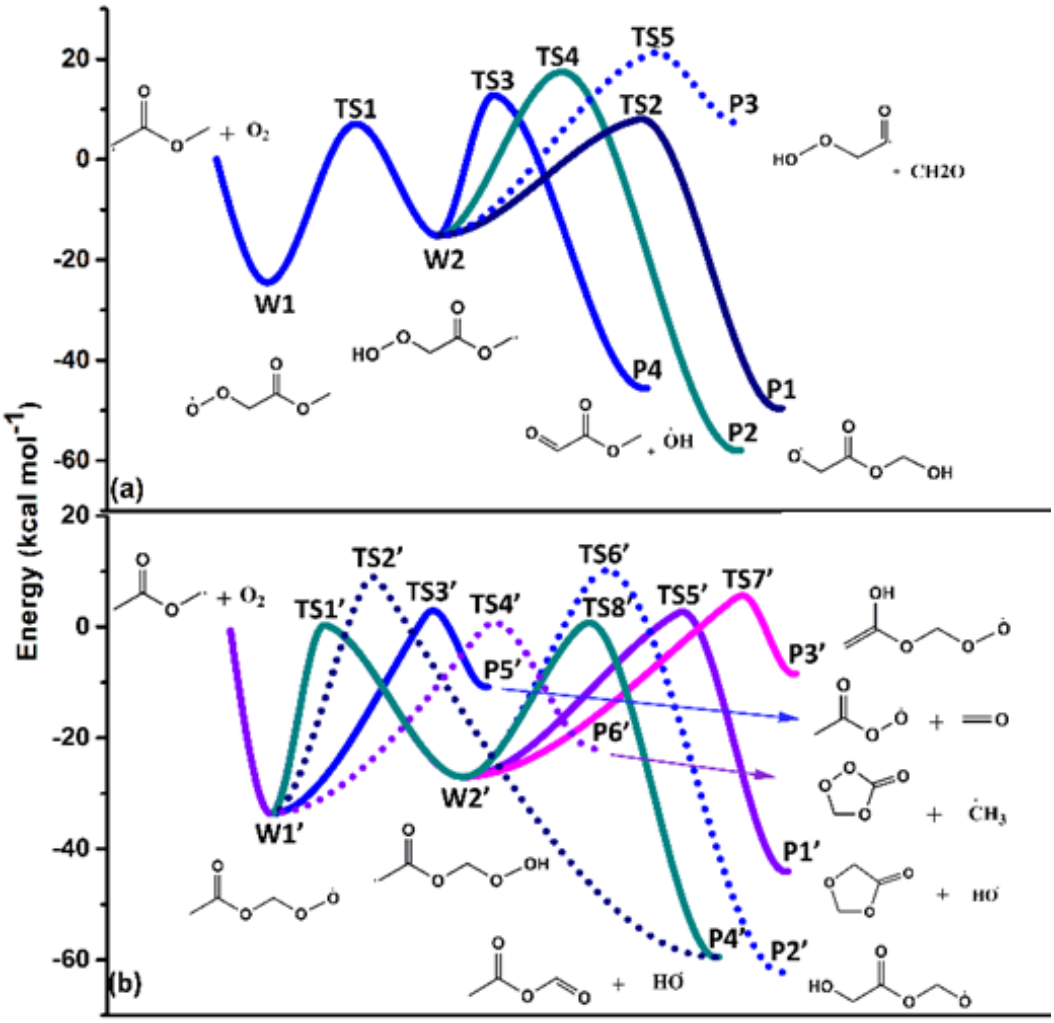

Fig.1. Potentials energy surfaces for the methyl acetate radicals with O_2 at the CCSD(T)/CBS//M06-2X/cc-pVTZ level (a) MA2J + O_2 , (b) MAMJ + O_2

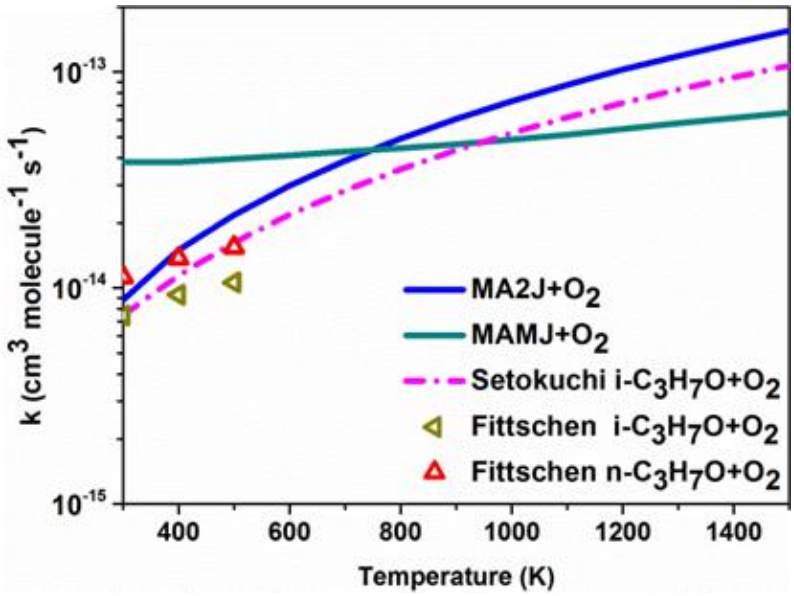

Fig.2. Rate constants for MA· +O_2→MAOO at high pressure limit (HPL). The HPL rate constants of the association reaction for chain-like alkoxy radicals are form previous study [43, 44].

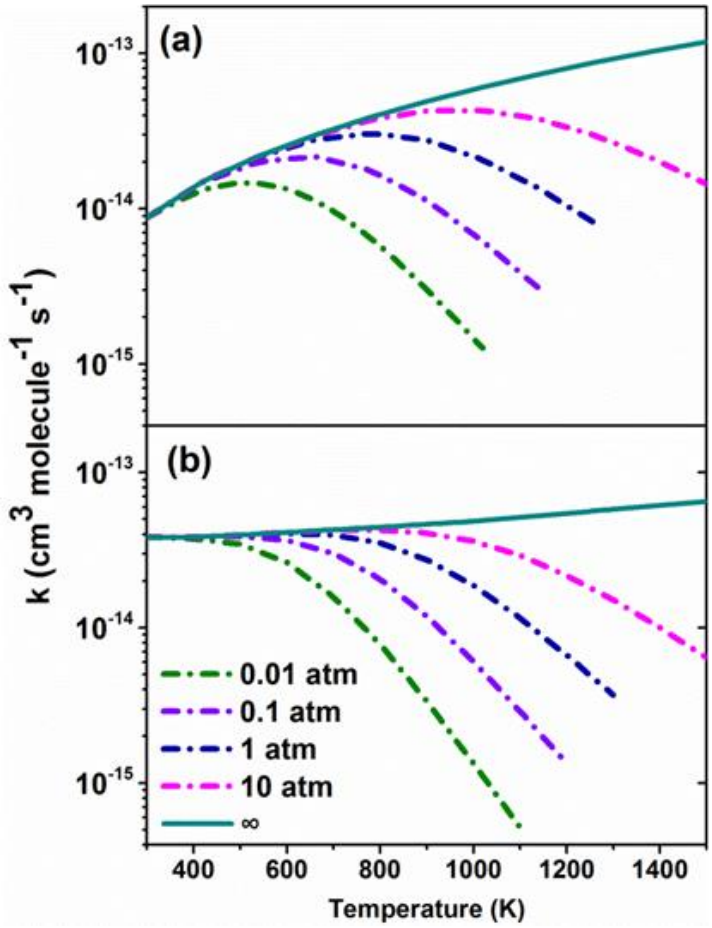

Fig. 3. Rate constants for MA· $+O_2 \rightarrow$MAOO at various T/P regimes. (a)·$CH_2C(=O)OCH_3$ + O_2 , (b) $CH_3C(=O)OCH_2$· + O_2

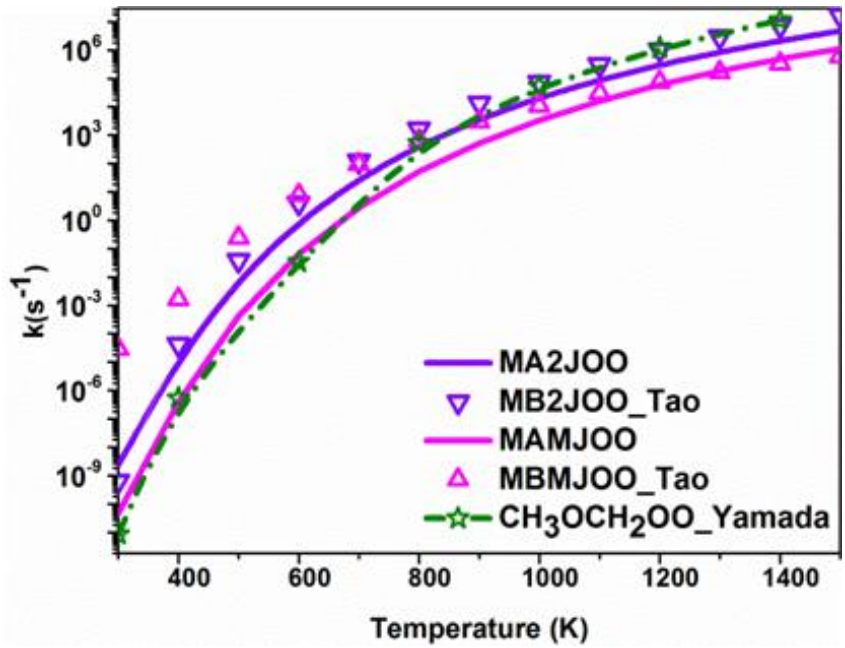

Fig.4. Rate constants of H-migration reactions for MAOO radicals at high pressure limit. The rate constants of isomerization for chain-like peroxyl radicals were shown in different symbols.

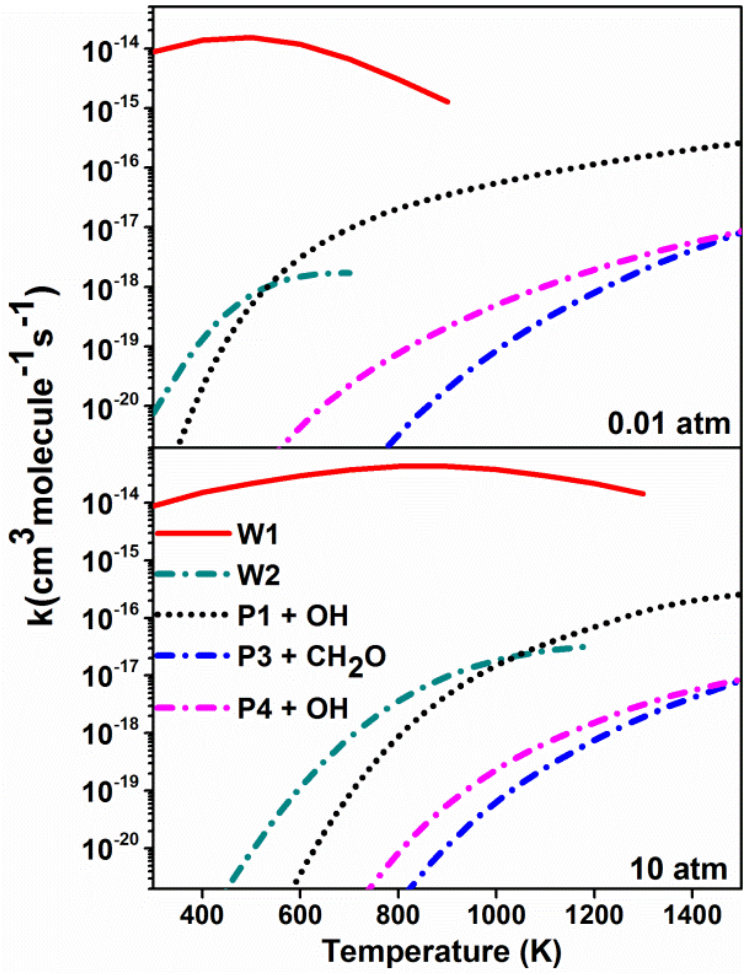

Fig.5. Rate constants for MA2J + O_2 → products in the temperature range of 300-1500K at 0.01atm and 10atm

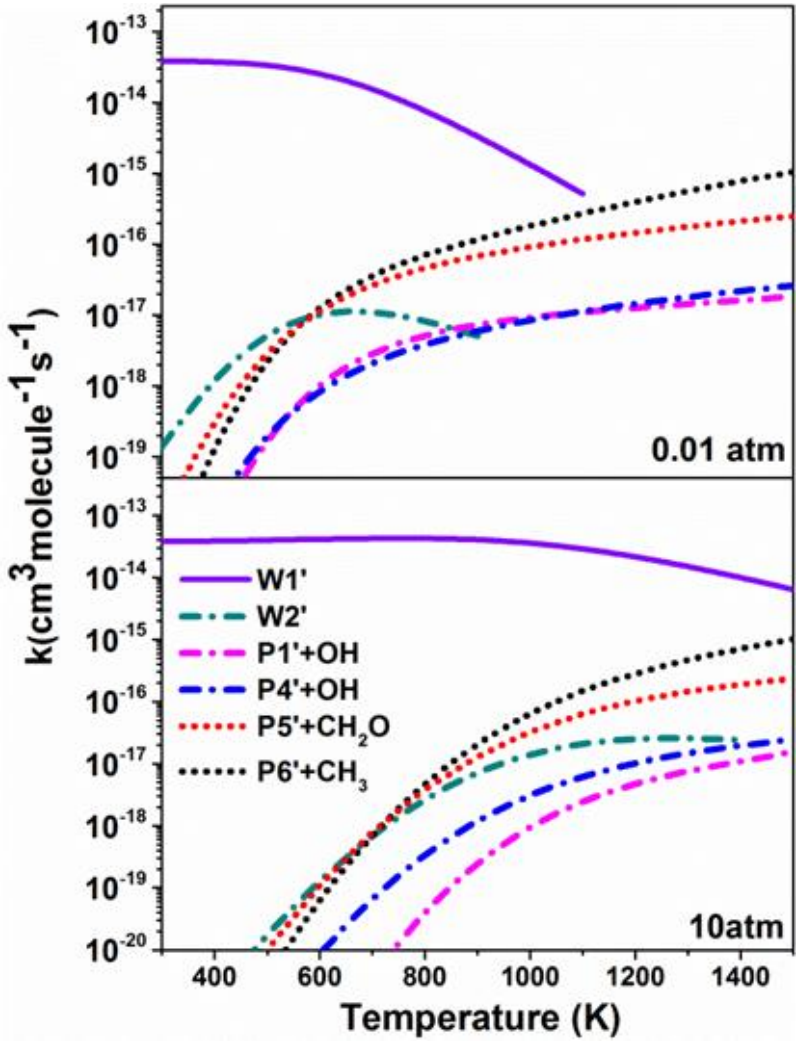

Fig.6. Rate constants or MAMJ + $O_2 \rightarrow$ products in the temperature range 300-1500K at 0.01atm and 10atm.